

Electron mobility in N-polar GaN/AlGaN/GaN heterostructures

Cite as: Appl. Phys. Lett. **93**, 042104 (2008); <https://doi.org/10.1063/1.2965483>

Submitted: 25 March 2008 . Accepted: 09 July 2008 . Published Online: 29 July 2008

David F. Brown, Siddharth Rajan, Stacia Keller, Yun-Hao Hsieh, Steven P. DenBaars, and Umesh K. Mishra



View Online



Export Citation

ARTICLES YOU MAY BE INTERESTED IN

N-polar GaN / AlGaN / GaN high electron mobility transistors

Journal of Applied Physics **102**, 044501 (2007); <https://doi.org/10.1063/1.2769950>

Model to explain the behavior of 2DEG mobility with respect to charge density in N-polar and Ga-polar AlGaN-GaN heterostructures

Journal of Applied Physics **120**, 115302 (2016); <https://doi.org/10.1063/1.4962321>

Polarization effects, surface states, and the source of electrons in AlGaN/GaN heterostructure field effect transistors

Applied Physics Letters **77**, 250 (2000); <https://doi.org/10.1063/1.126940>



Measure Ready
M91 FastHall™ Controller

A revolutionary new instrument
for complete Hall analysis

Lake Shore
CRYOTRONICS

Electron mobility in N-polar GaN/AlGaN/GaN heterostructures

David F. Brown,^{1,a)} Siddharth Rajan,¹ Stacia Keller,¹ Yun-Hao Hsieh,¹
Steven P. DenBaars,^{1,2} and Umesh K. Mishra¹

¹Electrical and Computer Engineering Department, University of California, Santa Barbara, California 93106, USA

²Materials Department, University of California, Santa Barbara, California 93106, USA

(Received 25 March 2008; accepted 9 July 2008; published online 29 July 2008)

The drift mobility of two-dimensional electron gasses in N-polar GaN/AlGaN/GaN heterostructures was measured with capacitance and resistance measurements using gated transmission line method structures. A decrease in mobility with increasing reverse bias of the gate was observed. A variational wave function was used to calculate the mobility limited by optical phonon, alloy disorder, and ionized impurity scattering as a function of gate bias, and found to match the experimental data well. Three distinct regimes where phonon, alloy, and impurity scattering are dominant were observed. © 2008 American Institute of Physics. [DOI: 10.1063/1.2965483]

N-polar GaN and its alloys are very promising due to the reversal of spontaneous and piezoelectric polarization charges at heterostructure interfaces.¹ In GaN/AlGaN/GaN structures, these polarization charges lead to a fixed sheet of mobile electrons, or a two-dimensional electron gas (2DEG), at the top heterointerface, which forms the basis of N-polar high electron mobility transistors (HEMTs).² Although N-polar HEMTs have been demonstrated,³⁻⁵ the transport properties have not been studied in great detail. Unlike Ga-polar HEMTs, the 2DEG charge is well confined in a deep triangular quantum well between the AlGaN barrier and a strong electric field induced by the surface potential. As the gate bias is increased, the electric field increases, confining the electrons further in the triangular potential well. The geometry of the electron wave function and its penetration into the barrier, both of which are of paramount importance to the transport properties of the 2DEG, are therefore strongly affected by the shape of the potential well.⁶ In this work, we create a theoretical model for calculating electron mobility in 2DEGs confined to triangular quantum wells as a function of the electric field in the well and apply it to N-polar HEMTs grown by metal-organic chemical vapor deposition (MOCVD). Charge and drift mobility were measured as a function of electric field using capacitance-voltage (*C-V*) measurements and gated transmission line method (TLM) structures and found to fit the theoretical calculations well.

The HEMT structure shown in Fig. 1 was grown by MOCVD on a sapphire substrate misoriented 3° toward the *a* plane using a growth technique detailed in an earlier study.³ The structure was capped with 5 nm of SiN grown by MOCVD in order to reduce gate leakage. Measurement of the drift mobility was done using gated TLM structures. The structures were aligned parallel to the surface steps because the drift mobility of N-polar HEMTs grown by MOCVD is anisotropic with respect to the direction of the source current.³ The resistance of TLM patterns with gate lengths varying from 2 to 20 μm, and access region lengths of 2 μm, was measured. The slope of the resistance line with respect to the gate length multiplied by the gate width gave the channel sheet resistance R_{sh} at each gate bias. A small

source current of 25 μA was used to avoid high-field effects and pinch off of the channel. The 2DEG sheet charge n_s as a function of gate bias was determined from capacitance-voltage measurements. The mobility was calculated by combining the two measurements using

$$\mu(V_G) = [eR_{sh}(V_G)n_s(V_G)]^{-1}. \quad (1)$$

A variational wave function for mobile electrons confined in a triangular quantum derived by Fang and Howard has had widespread use for electron transport calculations for 2DEGs in many different material systems.⁷ Traditionally, it has been assumed that the triangular potential well was shaped entirely by depleted background dopants and the mobile charge confined to the well. However, a previous experiment observed a strong impact on the mobility of 2DEGs when the electric field in the well is modulated by an external voltage.⁶ The structure used in this study is shown in Fig. 1. It consists of an Al_{0.33}Ga_{0.67}N barrier grown on a semi-insulating GaN buffer. The structure has a 5 nm GaN channel layer, a 25 nm Al_{0.1}Ga_{0.9}N cap layer, and a 5 nm SiN gate insulator on top of the barrier. Material properties for the alloys were determined using Vegard's law (Table I).

In a previous study, a variational wave function was derived for infinite triangular wells where F , the electric field, is known.⁸ A generalized form of the Fang-Howard wave function was used,

$$\psi(z) = Cz^a \exp(-bz/2), \quad z \geq 0, \quad (2)$$

where a and b are variational parameters, Γ is the gamma function, and $C = [b^{2a+1}/\Gamma(2a+1)]^{0.5}$. When $a=1$ this is identical to the Fang-Howard wave function. Using this as a trial function, one can obtain the first subband energy as

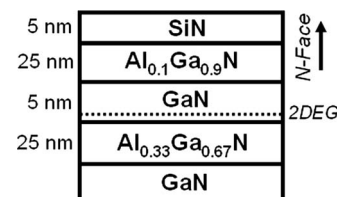


FIG. 1. Epitaxial structure of the N-polar HEMT used for both theoretical calculations and experimental measurements in this study.

^{a)}Electronic mail: dfbrown@ece.ucsb.edu.

TABLE I. Material constants for the device structure measured in this study.¹⁴

Property	Symbol	Value	Units
Effective mass (well)	m_w^*	0.20	...
Effective mass (barrier)	m_b^*	0.27	...
Conduction band offset (barrier-channel)	$\Delta E_{c,1}$	0.59	eV
Conduction band offset (channel-cap interface)	$\Delta E_{c,2}$	0.18	eV
Polarization charge (channel-cap interface)	$\sigma_{\pi,\text{net}}$	-0.0086	C/m ²
Static dielectric constant	ϵ	8.9	...

$$E_0 = \frac{\hbar^2}{2m_w^*} \frac{b^2}{4(2a-1)} + \frac{eF}{b}(2a+1). \quad (3)$$

Where m_w^* is the electron effective mass in the well, \hbar is the reduced Planck constant, and e is the electron charge. Minimization with respect to b yields the relation

$$b^3 = 4e\hbar^{-2}m_w^*F(2a+1)(2a-1) \quad (4)$$

for the variational parameter, and minimizing b yields $a = 1.5$. This wave function does not account for penetration of the wave function into the AlGaIn barrier, and thus cannot be used to calculate the alloy scattering rate. Furthermore, the centroid of the 2DEG is predicted to be further from the barrier, which can strongly affect some calculations.

We developed a modified form of this wave function in this study, which takes the form

$$\psi(z) = M \exp(\kappa_B z/2), \quad z < 0, \quad (5)$$

$$\psi(z) = NC(z+z_o)^a \exp(-bz/2), \quad z \geq 0, \quad (6)$$

where M and N are normalization constants and $z=0$ at the barrier-channel interface. In the barrier, κ_B is given by

$$\kappa_B = 2\hbar^{-1} \sqrt{2m_b^*(\Delta E_{c,1} - E_0)}, \quad (7)$$

where $\Delta E_{c,1}$ is the conduction band offset at the interface between the barrier and the channel layers and m_b^* is the electron effective mass in the barrier. Matching boundary conditions at $z=0$, z_o can be evaluated as

$$z_o = 2a(\kappa_B + b)^{-1}. \quad (8)$$

Applying the normalization boundary condition yields

$$N = \sqrt{\frac{\kappa_B}{\kappa_B e^{bz_o} + C^2 z_o^{2a}}}, \quad (9)$$

$$M = NCz_o^a, \quad (10)$$

which gives the electron wave function in closed form as a function of F .

Now only the electric field needs to be determined in order to know the wave function. Referring to the band diagram in Fig. 2, we obtained the expression

$$F_{\text{channel}} t_{\text{channel}} + F_{\text{cap}} t_{\text{cap}} = \phi_s + [E_0 + (E_F - E_0) - \Delta E_{c,2}]/e, \quad (11)$$

where Φ_s is the potential between the gate metal and the conduction band at the semiconductor-insulator interface, $\Delta E_{c,2}$ is the conduction band offset between the channel and cap layers, and E_0 is the energy of the first subband. Only the electric field in the channel layer is of interest, and using

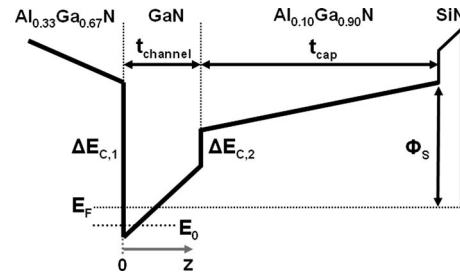


FIG. 2. Conduction band diagram of the HEMT used in this experiment. The N-polar surface is on the right hand side.

Poisson's equation we can substitute $F_{\text{cap}} = F_{\text{channel}} + \sigma_{\pi,\text{net}}/\epsilon$, where $\sigma_{\pi,\text{net}}$ is the net polarization charge at the cap channel and ϵ is the permittivity of GaN. Since the electric field must be known in order to calculate E_0 , we approximate E_0 as 0.15 eV for the purpose of calculating the electric field at zero gate bias. This was confirmed to be a good approximation by solving Schrodinger and Poisson's equations self-consistently. Expressed in terms of fundamental parameters, the electric field in the channel is

$$F(0) = \frac{\phi_s + \pi\hbar^2 n_s(0)/[em_w^*] + E_0(0)/e - \sigma_{\pi,\text{net}} t_{\text{cap}}/\epsilon - \Delta E_{c,2}/e}{t_{\text{channel}} + t_{\text{cap}}}, \quad (12)$$

if $E_f - E_0 \gg kT$. Φ_s was measured as 0.9 V for GaN in a previous experiment using C - V measurements,⁹ thus we used a value of 1 V for 10% AlGaIn. It follows that $F(V_g) = F(0) + V_g/(t_{\text{channel}} + t_{\text{cap}} + t_{\text{SiN}})$, where t_{SiN} is the thickness of the gate insulator. The charge in the channel will deplete as the gate is reverse biased. Using Poisson's equation, the channel charge at an arbitrary reverse bias is $n_s(V_g) = n_s(0) - \epsilon[F(V_g) - F(0)]/e$, where $n_s(0)$ was measured as $9.7e12 \text{ cm}^{-2}$ experimentally.

With the wave function and the charge density known, the mobility was calculated as a function of gate bias. The scattering mechanisms considered were polar optical phonon scattering,¹⁰ alloy disorder scattering,¹¹ and ionized impurity scattering from unintentional donors in the AlGaIn barrier layer,¹² of which we measured a concentration of $2.5e18 \text{ cm}^{-3}$ with secondary ion mass spectroscopy (SIMS) measurements. The high concentration of impurities in the barrier layer is due to the increased incorporation of oxygen during N-polar growth when compared to Ga-polar growth.¹³ This donor concentration was confirmed with C - V measurements.⁹ Impurities in other layers were not considered because the concentration of oxygen in the channel was measured as $1e17 \text{ cm}^{-3}$ by SIMS, and the increased distance of the wave function to the cap layer makes impurities in the cap layer insignificant compared to those in the barrier.

With the scattering rates known, the mobility is easily calculated using Matheson's rule and the Drude relation. Figure 3 shows the calculated mobility as a function of sheet charge in the channel and transverse channel electric field as the device is pinched off, along with the mobility limited by each of the scattering mechanisms. The mobility is limited by optical phonon scattering at low gate bias, but alloy scattering has an increasing impact as the barrier penetration of the wave function increases with increasing gate bias. As the field increases further, impurity scattering becomes the domi-

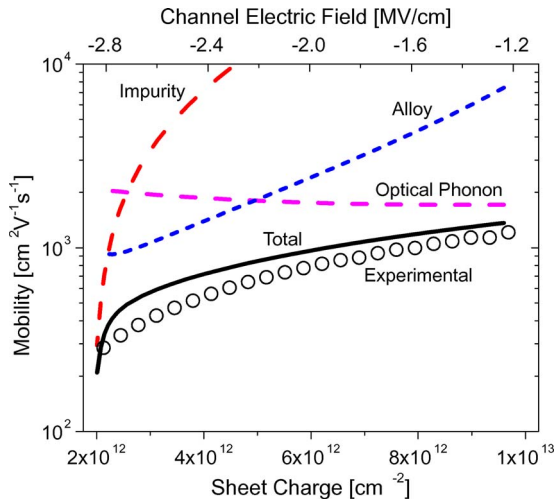


FIG. 3. (Color online) Theoretical calculations for mobility limited by optical phonon, ionized impurity and alloy disorder scattering, the total mobility, and the experimentally measured data plotted vs 2DEG sheet charge and channel electric field as the gate is pinched off.

nant scattering mechanism because the centroid of the 2DEG charge becomes very close to the ionized donors in the barrier, and screening is reduced due to the decrease in charge density. Both the shape and the values of the theoretical curve had a good fit to the data collected experimentally, although temperature-dependent measurements should be done to verify that impurity scattering is dominant near pinch off, as the 2DEG may be more weakly degenerate at lower charge densities and high temperature.

In conclusion, theoretical calculations for the mobility of electrons confined to a triangular well by an arbitrary electric field were done, and applied to an *N*-Polar HEMT. The drift mobility was measured with gated TLMs as a function of gate bias and found to match the experimental data well. It

was shown through theory and measurements that increasing the electric field in the channel of a 2DEG has a detrimental effect on the mobility because the wave function is pushed closer to the barrier alloy. This theoretical formalism can be applied to any other material system and device structure in which a 2DEG is confined to a triangular well by a strong electric field.

The authors gratefully acknowledge the support of AFOSR and the ONR-MINE program supervised by Dr. Paul Maki, Dr. Harry Dietrich, and Dr. Kitt Reinhardt.

- ¹F. Bernardini, V. Fiorentini, and D. Vanderbilt, *Phys. Rev. B* **56**, R10024 (1997).
- ²R. Dimitrov, M. Murphy, J. Smart, W. Schaff, J. R. Shealy, L. F. Eastman, O. Ambacher, and M. Stutzmann, *J. Appl. Phys.* **87**, 3375 (2000).
- ³S. Keller, C. S. Suh, Z. Chen, R. Chu, S. Rajan, N. A. Fichtenbaum, M. Furukawa, S. P. DenBaars, J. S. Speck, and U. K. Mishra, *J. Appl. Phys.* **103**, 033708 (2008).
- ⁴S. Rajan, A. Chini, M. H. Wong, J. S. Speck, and U. K. Mishra, *J. Appl. Phys.* **102**, 044501 (2007).
- ⁵M. H. Wong, S. Rajan, R. M. Chu, T. Palacios, C. S. Suh, L. S. McCarthy, S. Keller, J. S. Speck, and U. K. Mishra, *Phys. Status Solidi A* **204**, 2049 (2007).
- ⁶K. Hirakawa, H. Sakaki, and J. Yoshino, *Phys. Rev. Lett.* **54**, 1279 (1985).
- ⁷F. Fang and W. E. Howard, *Phys. Rev. Lett.* **16**, 797 (1966).
- ⁸B. Podor, CAS'95 Proceedings, Sinaia, Romania, 11–14 October 1995 (unpublished).
- ⁹Nidhi, S. Rajan, S. Keller, F. Wu, S. P. DenBaars, J. S. Speck and U. K. Mishra, *J. Appl. Phys.* **103**, 124508 (2008).
- ¹⁰B. L. Gelmont, M. Shur, and M. Strosio, *J. Appl. Phys.* **77**, 657 (1995).
- ¹¹G. D. Bastard, *Wave-Mechanics Applied to Semiconductor Heterostructures*, 1st ed. (Les Editions de Physique, Les Ulis Cedex, France, 1991).
- ¹²J. H. Davies, *The Physics of Low-Dimensional Semiconductors*, 1st ed. (Cambridge University Press, Cambridge, 1998).
- ¹³M. Sumiya, K. Yoshimura, K. Ohtsuka, and S. Fuke, *Appl. Phys. Lett.* **76**, 2098 (2000).
- ¹⁴NSM Archive—Physical Properties of Semiconductors (<http://www.ioffe.rssi.ru/SVA/NSM/Semicond/>), and references therein.